

## LA-UR-16-28619

Approved for public release; distribution is unlimited.

Title: High-Dose Neutron Detector Development Using  $^{10}\text{B}$  Coated Cells

Author(s): Menlove, Howard Olsen  
Henzlova, Daniela

Intended for: Report

Issued: 2016-11-08

---

**Disclaimer:**

Los Alamos National Laboratory, an affirmative action/equal opportunity employer, is operated by the Los Alamos National Security, LLC for the National Nuclear Security Administration of the U.S. Department of Energy under contract DE-AC52-06NA25396. By approving this article, the publisher recognizes that the U.S. Government retains nonexclusive, royalty-free license to publish or reproduce the published form of this contribution, or to allow others to do so, for U.S. Government purposes. Los Alamos National Laboratory requests that the publisher identify this article as work performed under the auspices of the U.S. Department of Energy. Los Alamos National Laboratory strongly supports academic freedom and a researcher's right to publish; as an institution, however, the Laboratory does not endorse the viewpoint of a publication or guarantee its technical correctness.

# **High-Dose Neutron Detector Development Using $^{10}\text{B}$ Coated Cells**

*Prepared for:*  
*U.S. Department of Energy*  
*Office of Nuclear Energy*  
*Materials Protection, Accounting and Control Technologies (MPACT)*

*Prepared by:*  
*H.O. Menlove and D. Henzlova*  
*Safeguards Science and Technology Group (NEN-1)*

*Los Alamos National Laboratory*  
*Los Alamos, NM 87545, USA*

*October 24, 2016*

LA-UR-xx-xxx

## 1. INTRODUCTION

The development of advanced sustainable nuclear fuel cycles relying on used nuclear fuel is one of the key programs pursued by the DOE Office of Nuclear Energy to minimize waste generation, limit proliferation risk and maximize energy production using nuclear energy. Safeguarding of advanced nuclear fuel cycles is essential to ensure the safety and security of the nuclear material. Current non-destructive assay (NDA) systems typically employ fission chambers or  $^3\text{He}$ -based tubes for the measurement of used fuel. Fission chambers are capable of withstanding the high gamma-ray backgrounds; however, they provide very low detection efficiency on the order of 0.01%. To benefit from the additional information provided by correlated neutron counting [1] higher detection efficiencies are required.  $^3\text{He}$ -based designs allow for higher detection efficiencies; however, at the expense of slow signal rise time characteristics and higher sensitivity to the gamma-ray backgrounds. It is therefore desirable to evaluate and develop technologies with potential to exceed performance parameters of standard fission chamber-based or  $^3\text{He}$ -based detection systems currently used in the NDA instrumentation.

Recent R&D efforts for nuclear safeguards applications in the area of  $^3\text{He}$ -free technologies have yielded a neutron detection system with performance characteristics similar to  $^3\text{He}$  tubes [2] that, in addition, offers features with the potential to outperform  $^3\text{He}$  tubes in applications that involve high gamma-ray dose and that require high count rates capabilities, such as spent fuel and pyro-processing measurements. The novel technology was developed by Precision Data Technology, Inc. (PDT) and is based on boron-lined parallel-plate proportional counters that are interleaved with high density polyethylene (HDPE) for optimum neutron moderation. The benefit of the technology lies in its inherent capability to sustain high count rates and in design features that allow minimizing its gamma-ray sensitivity and that allow for the capability to extract average neutron energy information from the multi-plate design. In addition, the boron-10 coated detector does not utilize  $^3\text{He}$  gas and as such provides a viable detection technology for  $^3\text{He}$ -replacement purposes.

The focus of the current research is to optimize the detector design for high count rates and high gamma-ray background applications. The key activities included MCNPX optimization of the detector design to maximize its neutron detection efficiency and the development of a fast amplifier with performance capability to match the detector fast rise-time signal characteristics. Significant progress has been made during the current year to increase the neutron counting efficiency by using new coating materials and procedures. The higher neutron efficiency allows for operating the detector in higher gamma fields at a reduced high voltage bias. Progress in this focus area is described in this report.

## 2. BORON-LINED PARALLEL-PLATE NEUTRON DETECTOR

The boron-lined parallel-plate technology developed for nuclear safeguards applications and manufactured by PDT consists of a detector module comprised of boron-lined parallel-plate detection cells. During the past two years, the detection cells have been improved by sealing them with welding and eliminating all organic material from the interior of the cells. This sealing method allows for high temperature treatment of the cells after the boron coating and out-gassing. The excellent efficiency stability with time and temperature change has been the benefit of the improvements.

The PDT corrugate cell design is illustrated in Fig. 1 where a detector pod would include multiple cells with HDPE layers between the cells. Typically there are 6-8 cells in a detector pod where the HDPE layers replenish the thermal-neutron population for each row of cells.

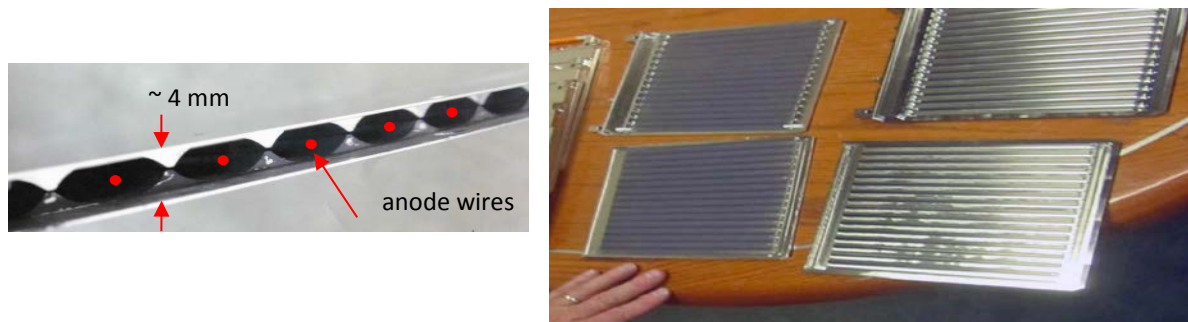


*Fig. 1. The PDT corrugated sealed cell cross-section and the open plates prior to sealing.*

Figure 2 shows the stack of cells in a neutron detector pod and the completed pod. The cells are filled with less than one bar of Ar+CO<sub>2</sub> gas for ionizing the charged particles from the neutron reaction in boron. The exterior can that holds the 6 cells is also filled with the same gas and pressure to isolate the interior cells from atmospheric pressure changes.

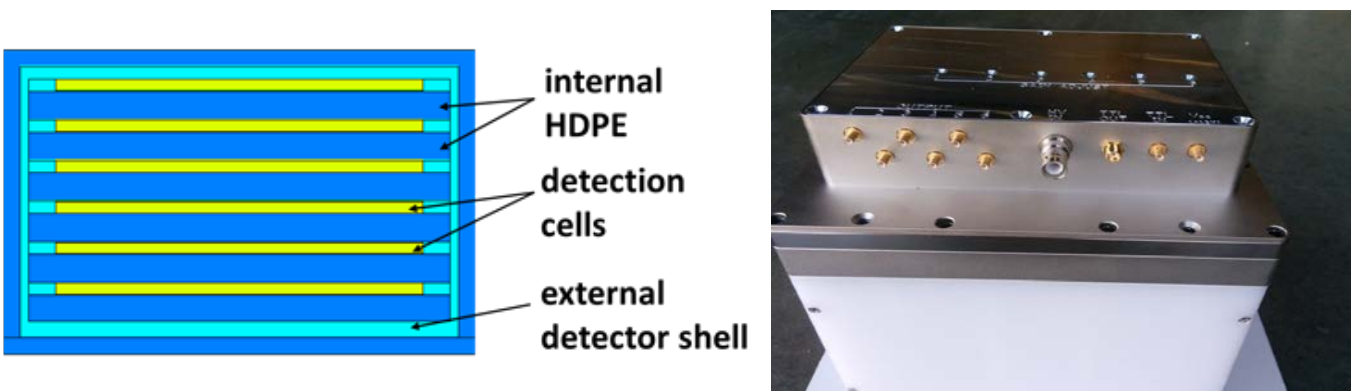


*Fig. 2. The PDT corrugated sealed cell stack and the amplifier junction box.*

### 3. BORON COATING EFFICIENCY IMPROVEMENTS

The ability to measure neutrons in the presence of high gamma-ray backgrounds depends on the detector design, the neutron efficiency, and the amplifier characteristics. The advanced material coating procedure at PDT has provided higher efficiency for neutron counting and better gamma rejection compared with their past systems. The improved efficiency of the new boron coating procedures was tested by a series of measurements at LANL using the new plate coatings compared with the prior coatings. The comparisons were for individual boron coated plates as well as sealed-cells (two plates). The individual plate comparison gave an improvement in efficiency of a factor of 1.5. The sealed-cells allow heat treatment to remove all organic impurities.

Measurements of the improved coating materials were also made with PDT  $^{10}\text{B}$  coated plates that could be easily installed into the original PDT 12" tall detector pod [3]. For the initial tests, the 6 cell pod was loaded with a new test cell in the front position (cell-1) followed by a standard cell with HLNb [4] type coating in the second position (cell-2), and the other 4 cells had blank loadings. The measurements were made with a  $^{252}\text{Cf}$  source placed next to the front surface or side of the pod. The neutron counting rates were measured to better than 0.5% precision, and the rates are relative to each other and not absolute.

Figure 3 shows the results of the measurements where a  $^{252}\text{Cf}$  source was scanned along the side of the pod that contained the new cell-1, as well as an older type cell-2. The HDPE moderator for the pod was arranged to have equal moderator for both cells. Thus, the counting rate difference of a factor of 1.5 shows the improved efficiency of the new type PDT boron coated cells.

The experiment was repeated with the  $^{252}\text{Cf}$  scan on the opposite side of the pod to show the uniformity of the boron coating material. The offset of the two peaks of 0.6" (1.5 cm) represents the separation of the two cells in the detector pod.

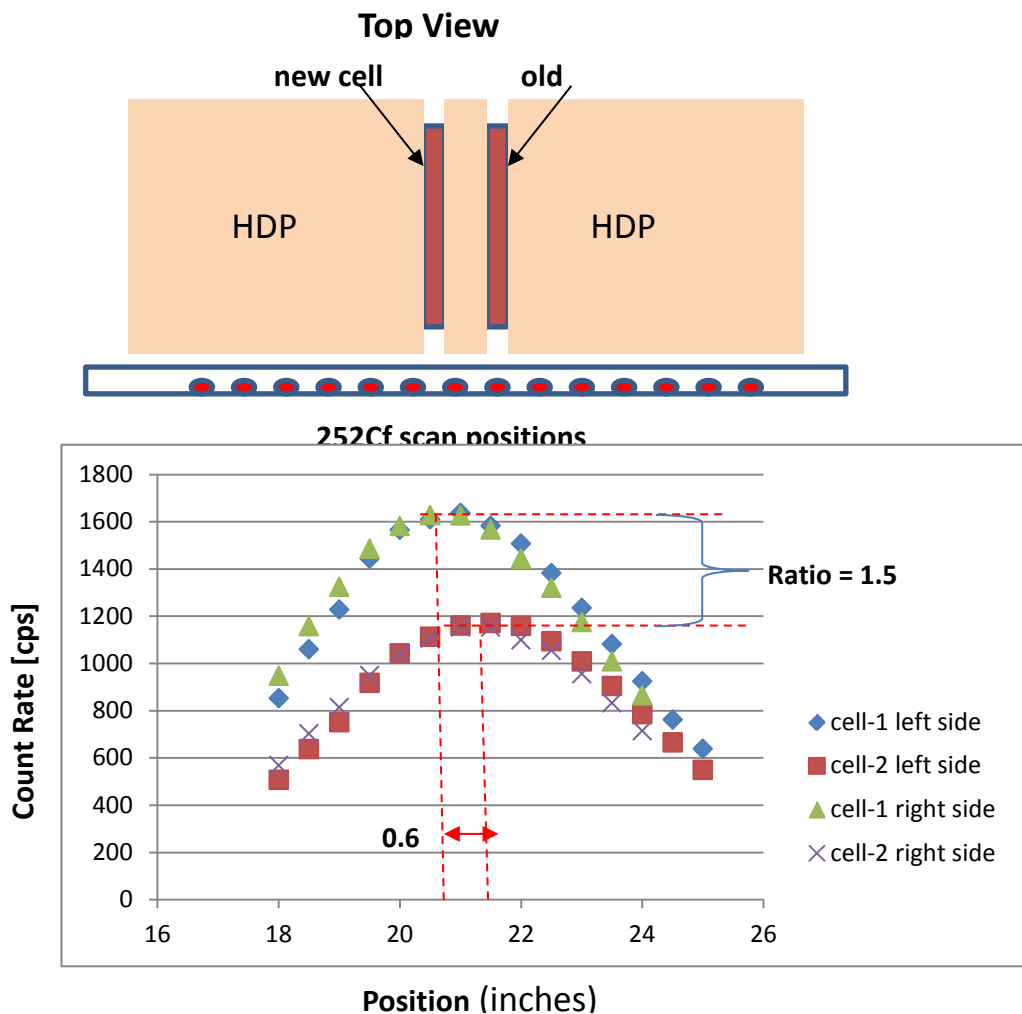


Fig. 3. Scan profiles for a  $^{252}\text{Cf}$  point source with movement along both sides of the detector pod that had symmetric HDPE moderator on both sides of the 2 cells.

Of key interest in the detectors to replace  $^3\text{He}$  for safeguards measurements, is the doubles rate error for coincidence counting. This error can be measured by the standard deviation of the doubles scatter in repeat measurements of the same sample where the relative error represents a comparison of the two cells used for Fig. 3. For the coincidence counting purpose, we measured a  $^{252}\text{Cf}$  source that was positioned on the side of the detector pod and midway between cell-1 and cell-2. The HDPE was configured as described above to provide equal thermal-neutron flux to both cells. The repeat runs had 35 cycles, 30 s each, for both cells with

the doubles rates being collected in a JSR-15 shift-register with a 128 us gate. The data from the measurement is shown in Table 1.

**Table 1. Measured data for a two cell pod with cell-1 having the improved boron coating and cell-2 having the original coating.**

<sup>252</sup> Cf Source on Side of Pod	cell #	Time [s]	S [cps]	D [cps]	error [cps]	D [%]	Ratio S <sub>1</sub> /S <sub>2</sub>	Ratio D <sub>1</sub> /D <sub>2</sub>	FOM ratio
12" Pod with symmetric poly	2	35x30	3073	13.92	1.16	8.35	1.00	1.00	1.00
12" Pod with symmetric poly	1	35x30	4750	47.77	1.65	3.46	1.55	3.43	<b>2.41</b>

An important result in this test program was that the singles rate increased by a factor of 1.55 and the doubles rate increased by a factor of 3.45. The doubles rate increase is greater than the square of the singles increase because the die-away time of the new cells is shorter than for the original cell, and this increase the coincidence gate fraction [1] for the new cells. The figure of merit (FOM) was defined as the reduction in the doubles rate statistical error for cell 1 vs. cell 2.

#### 4. PROCUREMENT OF AN OPTIMIZED DETECTOR POD

The MCNP optimization study from our prior report [5] was used to specify a new detector pod to be fabricated at PDT that had six corrugated sealed-cells. The HDPE thickness between the cells was 16 mm. The outer dimensions of the detector moderator are 20x20x16 mm with a total height of 250 mm. We have referred to the new detector as the 8" pod to distinguish it from prior systems that were 12" tall. Figure 4 shows the detector module including the internal cells.

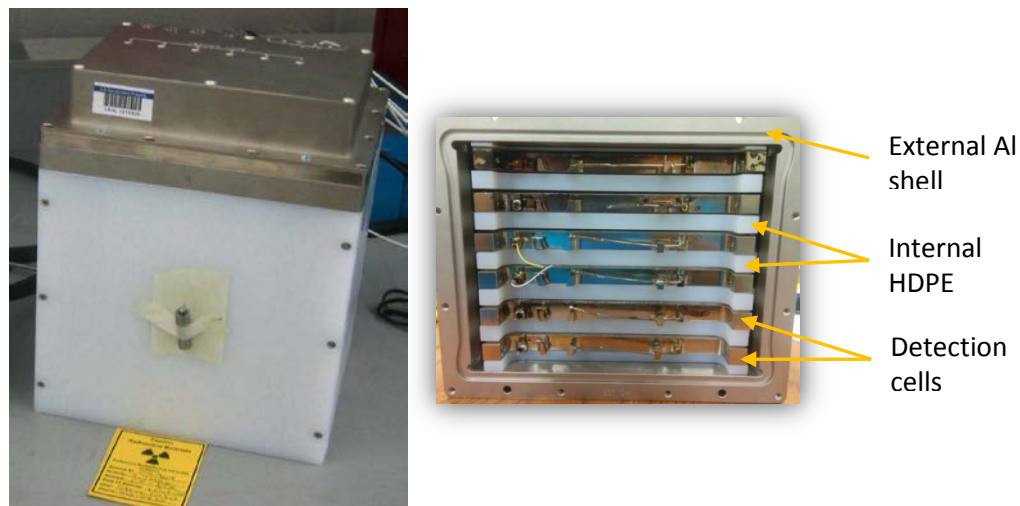


*Fig. 4. PDT 8" detector pod with 6 sealed corrugated cells with HDPE plates between cells*



The 8" detector was fabricated with the new PDT fast-amplifier on each cell to provide List mode output for each cell. The TTL outputs from the 6 cells are shown in Fig 5. The outputs also include the OR'ed sum of the 6 cells to be a convenient TTL signal for input to a JSR-15 coincidence module. The amplifiers provide external screws for gain and threshold adjustments. There are LED lights on each amplifier to indicate a pulse event that is above threshold.

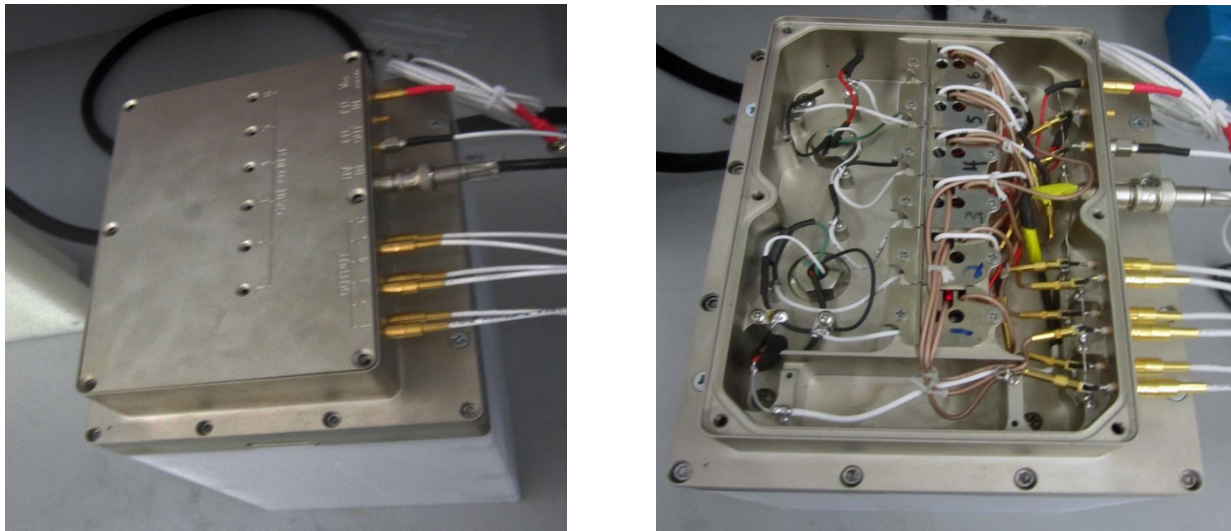


*Fig. 5. PDT 8" detector pod with 6 sealed corrugated cells and 6 PDT fast amplifiers with list mode TTL outputs from each of the amplifiers.*

## 5. TEST RESULTS FOR THE 8" DETECTOR

The initial measurements to evaluate the 8" PDT detector consisted of high voltage (HV) plateaus for each amplifier-cell channel. The thresholds and gains can be set using the plateaus. Figure 6 shows the HV plateaus in the region from 600-1200 V. We observed that the plateaus are noise free up to 1200 V, and we used an operating HV of 1140 V for operation in low activity gamma fields. All of the outputs were measure with a pulse train recorder (PTR) to show that there was no double pulsing in the neutron counts.

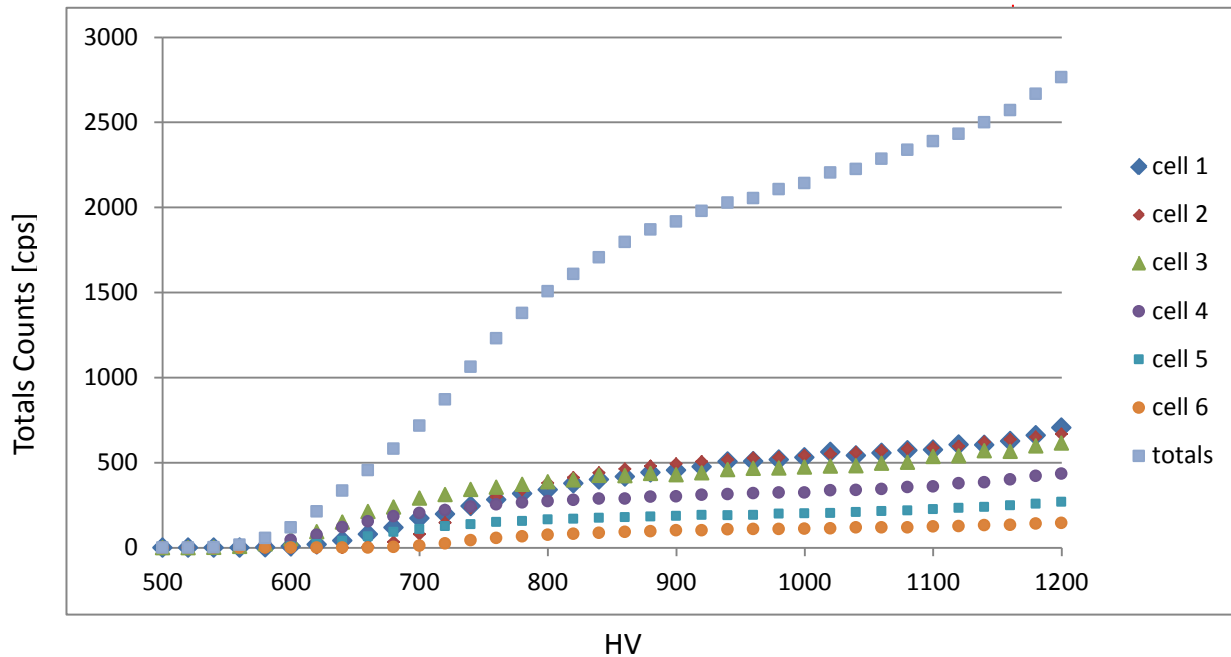


Fig. 6. Plateau curves the 6 cells and the total rate for the PDT 8'' detector pod.

The relative efficiency was measured using a calibrated  $^{252}\text{Cf}$  source with the source taped to the detector face and also at a separation distance of 50.8 cm. Table 2 presents the results together with a comparison with typical six tube  $^3\text{He}$  slab detectors. Figure 7 shows the two detectors that were used for the efficiency comparison.

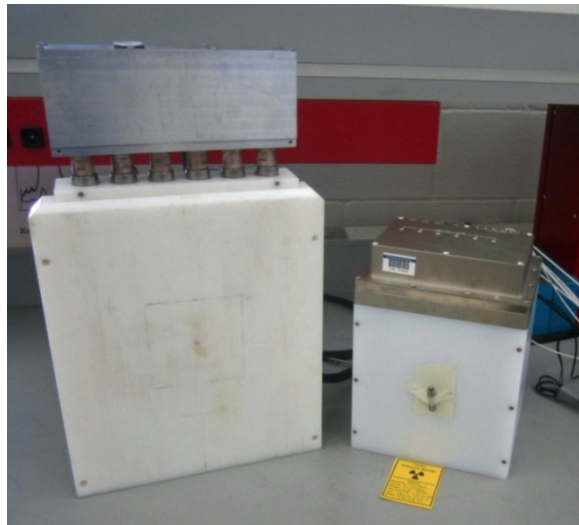


Fig. 7. A photo of the 8'' pod next to a six tube  $^3\text{He}$  slab detector.

**Table 2. Measured data for the comparison of the 8" PDT boron plate detector with two UNCL type slab detectors ( $^{252}\text{Cf}$  source F4-964 @ 64,946 n/s on 7/27/2016)**

Detector	Face Area [cm <sup>2</sup> ]	Active Area [cm <sup>2</sup> ]	Contact Rate [cps]	50cm Rate [cps]	Contact Rate per cm <sup>2</sup>	50 cm Rate per cm <sup>2</sup>	50 cm Rate per active cm <sup>2</sup>
8" PDT Pod "updated"	413	234	2754	71.8	7.69	0.174	0.307
Prototype UNCL slab	1039	733	4742	213.7	4.57	0.249	0.292
Antech 56 slab	1086	776	4582	208.2	4.23	0.234	0.268

The different dimensions of individual slabs require corrections for comparing the counting rates. For a 50.8 cm distant neutron source in front of the face of the detector, the number of neutrons hitting the detector face is proportional to the face area. The HDPE face area for the collar is 1039 cm<sup>2</sup>, and 1086 cm<sup>2</sup> and 413 cm<sup>2</sup> for the prototype UNCL slab [6], Antech 56 slab and  $^{10}\text{B}$  slab, respectively. The corresponding active area was estimated as 733 cm<sup>2</sup>, 776 cm<sup>2</sup> and 234 cm<sup>2</sup> for the prototype UNCL slab, Antech 56 slab and  $^{10}\text{B}$  slab, respectively. The intrinsic efficiency is then the counting rate per square cm per neutron on the face. This intrinsic efficiency is also dependent on the detector size where the larger size provides a higher intrinsic efficiency because there is less neutron loss from perimeter leakage.

Figure 8 illustrates the relative intrinsic efficiency of the 3 detector slabs where the rates have been normalized to the active counting area in each slab. The prototype UNCL has a slightly higher counting efficiency per active area than the new Antech 56 slab because of the 6 bar  $^3\text{He}$  pressure in the prototype detector versus 4 bar in the Antech 56 detectors. The face area of the Antech 56 detector is taller than for the prior designs because of the added height from the HN connectors to provide the removable tube feature. The 8" PDT boron-10 detector had a slightly higher efficiency per cm<sup>2</sup> of active area than either of the  $^3\text{He}$  tube models.

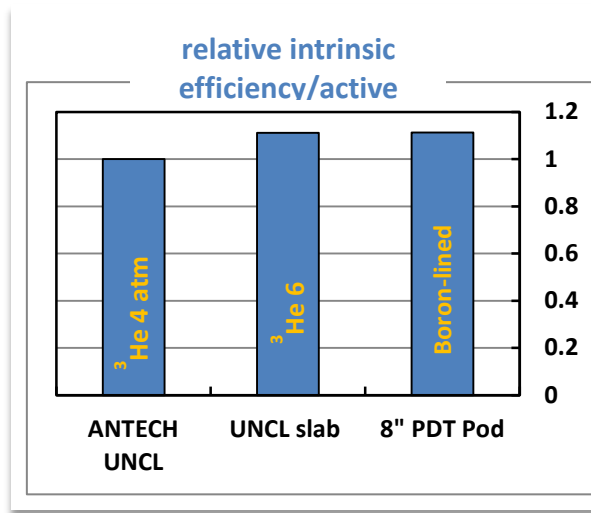


Fig. 8. The efficiency comparison of the 8" PDT boron-10 pod with the six tube  $^3\text{He}$  slab detectors containing  $^3\text{He}$  gas at 4 and 6 bar pressure.

## 6. INITIAL HIGH DOSE GAMMA TESTS

Prior to performing the high dose gamma-ray measurements, it was necessary to adjust the amplifier gains and thresholds on each of the cells for the 8" detector for optimum gamma rejection. This activity was performed in the laboratory using two  $^{137}\text{Cs}$  sources that had a combined contact dose of  $\sim 100$  mR/h. The procedure was to measure the HV plateau with the  $^{137}\text{Cs}$  placed in contact with the front face of the detector. The amplifier gain was then adjusted so that the gamma pileup was just starting at a HV setting of 1000V for each of the detector cells. At the adjusted gain settings, the HV plateaus were measured for each amplifier both with and without a  $^{252}\text{Cf}$  source (A7-866) attached to the face of the detector pod. The plateau curves were also measured for the totals rate from the  $^{252}\text{Cf}$  source without the  $^{137}\text{Cs}$  source.

Figure 9 shows the HV plateau curves for the  $^{252}\text{Cf}$  source, the  $^{137}\text{Cs}$  source, and the combined  $^{252}\text{Cf}$  and  $^{137}\text{Cs}$  sources. We see that the  $^{252}\text{Cf}$  counting rate is not impacted by the  $^{252}\text{Cf}$  gamma emission over the entire plateau, and the pileup of gammas from the  $^{137}\text{Cs}$  at 100 mR/h is apparent at  $\sim 1000$  V. Figure 10 shows the gamma pileup thresholds for all 6 cells where the gains have been adjusted to have the gamma threshold at  $\sim 1000$  V. The corresponding neutron thresholds were at  $\sim 660$  V. Cell-1 was missing from the plateau curves because of an amplifier gain malfunction.

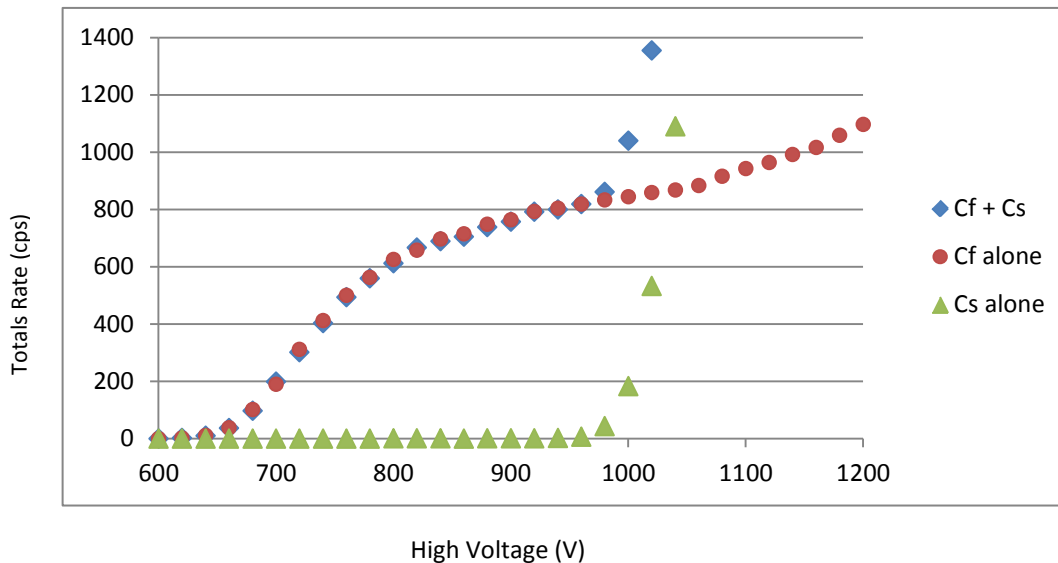


Fig. 9. High voltage plateau curves for the totals rate from the 8' detector for  $^{252}\text{Cf}$  and the combined  $^{252}\text{Cf}$  (44,800 n/s) and  $^{137}\text{Cs}$  sources (100 mR/h).

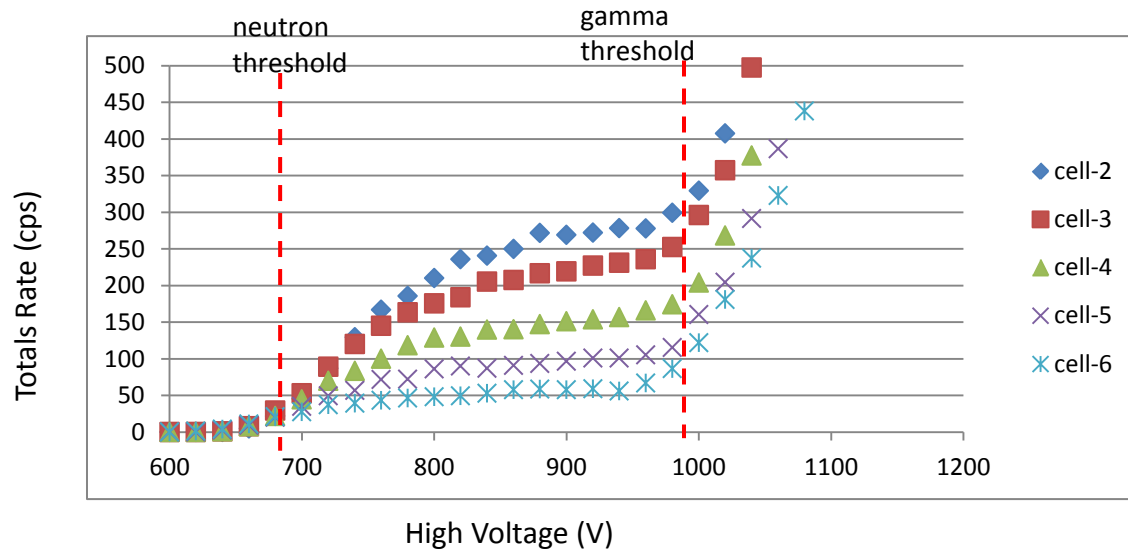


Fig. 10. High voltage plateau curves for the counting rate from each of the 6 cells for the combined  $^{252}\text{Cf}$  and  $^{137}\text{Cs}$  sources.

For the initial high dose gamma tests of the 8" pod, we made use of the 4.5 Ci  $^{226}\text{Ra}$  source in the shielded cell at LANL, TA-35, building 27. The source provides high energy gamma rays ( $\sim 0.8$  MeV average energy) with dose levels from 1-150 R/h depending on distance from the source. A photo of looking through the hot-cell window of the  $^{226}\text{Ra}$  source and the 8" detector is shown in Fig 11, and the gamma dose versus separation distance is on the right.

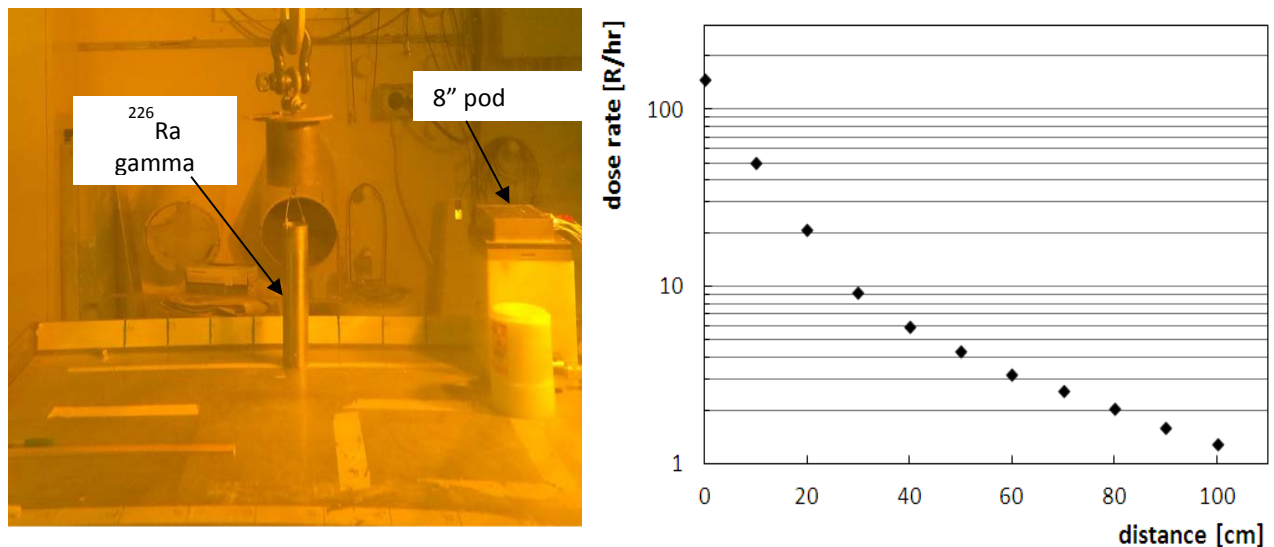


Fig. 11. Photo through the hot-cell widow of the  $^{226}\text{Ra}$  source during the high dose measurements for the PDT detector pod (left), and the gamma dose versus distance curve (right)

## 7. GAMMA REJECTION VIA NEUTRON EFFICIENCY INCREASE

We note from the Plateau curve in Fig. 9 that the change in HV in going from a very small gamma dose (eg.  $^{252}\text{Cf}$ ) at 1140V to a dose of  $> 100$  R/h is at  $\sim 900$  V. The corresponding loss of neutron efficiency was only  $\sim 25\%$ ; however, the gain in gamma resistance was several orders of magnitude. The improvements in the boron-10 coating technology at PDT during 2016 provided an increase in neutron efficiency of about a factor of 1.5 for the same size back-plate for the boron coating. Thus, the gain in gamma rejection for the same neutron efficiency is more than 4 orders of magnitude. Note that if the efficiency gain comes from an increase in the back-plate area, the gamma pileup will increase faster than the increase in the neutron counting efficiency! Thus, the gamma resistance is dependent on the area of the back-plate that is coated with the boron. The improved neutron efficiency for the PDT plates was accomplished without any increase in the area of the coating back-plate.

## 8. CONCLUSIONS

During FY16 the boron-lined parallel-plate technology was optimized to fully benefit from its fast timing characteristics in order to enhance its high count rate capability. To facilitate high count rate capability, a novel fast amplifier with timing and operating properties matched to the detector characteristics was developed and implemented in the 8" boron plate detector that was purchased from PDT. Each of the 6 sealed-cells was connected to a fast amplifier with corresponding List mode readout from each amplifier.

The FY16 work focused on improvements in the boron-10 coating materials and procedures at PDT to significantly improve the neutron detection efficiency. An improvement in the efficiency of a factor of 1.5 was achieved without increasing the metal backing area for the boron coating. This improvement has allowed us to operate the detector in gamma-ray backgrounds that are four orders of magnitude higher than was previously possible while maintaining a relatively high counting efficiency for neutrons. This improvement in the gamma-ray rejection is a key factor in the development of the high dose neutron detector.

## 9. REFERENCES

- [1] D. Reilly, N. Ensslin, and H. Smith, Jr., "*Passive Nondestructive Assay of Nuclear Materials*", Los Alamos National Laboratory Technical Report LA-UR-90-732 (1991).
- [2] D. Henzlova, L.G. Evans, H.O. Menlove, M.T. Swinhoe, V. Henzl, C. Rael, I. Martinez and J.B. Marlow, "*Results of the Evaluation and Comparison of Alternative Neutron Detectors for Potential  $^3\text{He}$  Replacement for Nuclear Safeguards Applications*", LANL report, LA-UR-12-00837 (2012)

[3] D. Henzlova and H.O. Menlove, *“Integrated Test and Evaluation of  $^3\text{He}$  Replacement Technologies for Safeguards and Nonproliferation Applications – boron-based HLNC-B counter build”*, Los Alamos National Laboratory Report LA-UR-13-27499 (2013).

[4] Menlove H.O., Swansen J.E.; *“A high-performance neutron time correlation counter”*, Nuclear Technology 71, 497, 1985

[5] D. Henzlova et al.: *“Integrated Test and Evaluation of  $^3\text{He}$  Replacement Technologies for Safeguards and Nonproliferation Applications – boron-based HLNB counter field trial”*, LANL report, LA-UR-15-27844 ver. 3 (2015)

[6] Menlove, H.O., J.E. Stewart, S.Z. Qiao, T.R. Wenz, G.P.D. Verricchia, *“Neutron Collar Calibration and Evaluation for LWR Fuel Assemblies Containing Burnable Neutron Absorbers.”* United States Program for Technical Assistance to IAEA Safeguards, Los Alamos National Laboratory. LA-11965-MS. 1990